3.2.3 SIMULTANEOUS ROCKET AND MST RADAR OBSERVATION OF AN INTERNAL GRAVITY WAVE BREAKING IN THE MESOSPHERE

Steven A. Smith* and David C. Fritts

Department of Physics, Geophysical Institute
University of Alaska
Fairbanks, AK 99701

Ben B. Balsley

Aeronomy Laboratory
National Oceanic and Atmospheric Administration
Boulder, CO 80303

C. Russell Philbrick

Air Force Geophysics Laboratory
Hanscom AFB, MA 01731

INTRODUCTION

In June, 1983, the STATE (Structure and Atmospheric Turbulence Environment) rocket and Poker Flat MST radar campaign was conducted to measure the interaction between turbulence, electron density and electron density gradient that has produced unusually strong MST radar echoes from the summer mesosphere over Poker Flat, Alaska (PHILBRICK et al., 1984). During the campaign, the Poker Flat MST radar was operating with a spatial resolution of 300 m and a time resolution of 1 1/2 to 3 minutes to obtain radial wind velocities along a vertical beam and two oblique beams directed 15° off-zenith and toward azimuths of 334°E (the 'north' beam) and 64°E (the 'east' beam). Several rocket salvos were launched consisting of passive spheres, electron density probes and accelerometers. In this paper, we present the analysis of radar wind measurements and a concurrent wind and temperature profile obtained from a rocket probe carrying a three-axis accelerometer. The two data sets provide a fairly complete (and in some cases, redundant) picture of the breaking (or more correctly, the saturation) of a large-amplitude, low-frequency, long-wavelength internal gravity wave. The data show that small-scale turbulence and small-scale wave intensity is greatest at those altitudes where the large-scale wave-induced temperature lapse rate is most negative or most nearly unstable, but the wind shear due to the large-scale wave is a minimum.

A brief review of linear gravity-wave theory will be presented in the next section as an aid to the identification of the gravity-wave signature in the radar and rocket data. A more complete review of gravity-wave saturation theory can be found in FRITTS (1984). Analysis of the time and height cross sections of wind speed and turbulence intensity observed by the Poker Flat MST radar will follow. Then, the vertical profile of temperature and winds measured by a rocket probe will be examined. Finally, the use of the independent but complimentary data sets provided by the rocket and the radar will be discussed and implications for theories of wave saturation will be presented.

*Currently at the Cooperative Institute for Research in Environmental Sciences (CIRES), University of Colorado, Boulder, CO.

ABBREVIATED GRAVITY-WAVE THEORY

Application of the linear perturbation method to the equations of motion, continuity and thermodynamic energy produces gravity-wave solutions with waves of the form $e^{z/2H} e^{-i(kx + mz - kct)}$ where H is the density scale height, k ($= 2\pi/\lambda_x$) and m ($= 2\pi/\lambda_z$) are horizontal and vertical wave numbers, c ($= w/k$) is horizontal phase speed and x, z and t represent horizontal and vertical distances and time. For simplicity, it is assumed that the wave is propagating in the x direction. The $e^{z/2H}$ factor maintains a constant energy flux for waves propagating vertically through the atmosphere with density decreasing exponentially with height. Mean quantities will be denoted by overbars, perturbation quantities will be primed and subscripts (except on λ) will represent derivatives with respect to the subscript.

Substituting solutions of this form in the equations yields a dispersion relation

$$m = \frac{N}{\bar{u}-c} \tag{1}$$

where N is the Brunt-Vaisala frequency defined by $N^2 = \frac{g}{\theta}\frac{\partial\theta}{\partial z}$ (g is the acceleration due to gravity and θ is potential temperature) and $\bar{u}$ is the mean horizontal wind in the direction of wave propagation. This is a simplified dispersion relation obtained by assuming an intrinsic frequency, w ($= k(\bar{u}-c)$), far from the inertial frequency, f, and from N, or $f << w << N$, assuming that the waves are hydrostatic (i.e., $k << m$) and also by neglecting vertical shear of the horizontal wind and neglecting terms of the order of $1/4H^2$ which implies that $\lambda_z < 4\pi H \sim 90$ km. The approximate dispersion relation yields an estimate of $\bar{u}-c$ from measurements of N and vertical wavelength.

Since radars and rockets measure two orthogonal, horizontal wind components and temperature, relations between these variables are needed to concisely identify a gravity wave. A relation between horizontal and vertical velocity perturbations comes from the continuity equation

$$u' = -\frac{m}{k} w' \tag{2}$$

u' and v' (the transverse wind component) are related by

$$v' = \frac{if}{w} u' \tag{3}$$

which comes from solution of the horizontal component equations of motion. This relation demonstrates that as w approaches f, the transverse wave perturbation component increases and the perturbation velocity vector traces out an ellipse. Such elliptical waves are known as inertio- or rotary-gravity waves.

Finally, from the thermodynamic energy equation relations for temperature perturbations are obtained:

$$\theta' = -i\frac{u'\bar{\theta}_z}{N} \qquad T' = -i\frac{u'\bar{T}_z}{N} \tag{4}$$

With these relations for temperature variables, a saturation limit on wave amplitude can be obtained. When, $(\bar{\theta} + \theta')_z < 0$ or $\theta_z' \leq -\bar{\theta}_z$ the atmosphere is convectively unstable. Taking derivatives gives

$$\frac{mu'}{N}\bar{\theta}_z \leq -\bar{\theta}_z \tag{5}$$

substituting for $m = N/\bar{u}-c$ we obtain

$$|u'| \geq |\bar{u} - c| \tag{6}$$

Thus, whenever the wave perturbation velocity exceeds the intrinsic wave phase speed, convective instabilities are initiated in that portion of the wave field where $\theta_z' \leq -\bar{\theta}_z$ which also corresponds to that point in the wave field where u' is maximum in the direction of wave propagation. Thus, the wave breaks down where the velocity perturbation is a maximum and the shear is a minimum. In the case of rotary waves, there is a shear of the transverse component at the point where u' is maximum. This transverse shear contributes to lowering the local Richardson number and instabilities can develop at amplitudes smaller than $\bar{u}-c$ (FRITTS and RASTOGI, 1985).

From the above discussion, a possible scenario for a propagating wave is that it will grow in proportion to $e^{z/2H}$ as it ascends until it reaches the saturation amplitude of $\bar{u}-c$. At that height, turbulence will be produced by instabilities, which will prevent the wave from growing further and hence the wave amplitude will be fixed at the saturation amplitude. This scenario was originally proposed by HODGES (1967).

Wave structure will be determined using the above relations and different aspects of the data. From both the rocket and radar measurements of the horizontal winds, the direction of wave propagation can be obtained. Both radar and rocket data yield estimates of the vertical wavelength and thus approximate intrinsic phase speeds from equation 1. Then it is possible to check the saturation condition with equation 6. The rocket probe provides an additional check on the saturation condition since θ' and θ_z' can be observed.

POKER FLAT MST RADAR DATA

The horizontal winds observed by the Poker Flat radar near the mesopause on June 15, 1983, are shown in Figure 1. The plotted vectors are computed from 15-minute averages of the oblique, radial winds that have been converted to horizontal by assuming the vertical wind is zero for a 15-minute average. Notice also, that only measurements at locations where the signal was significantly above the noise floor were used in the averages. Thus, it is possible to see two regions of strong signal propagating downward with time near 1400 and 2100 AST (Alaska Standard Time) which are separated by a blank region of no signal. This blank region implies either that the 3 m (radar half wavelength) component of turbulence was weak or that the electron-density gradient was weak or both.

The wind pattern in the latter half of the day reveals the presence of an inertio-gravity wave since the wind vectors rotate clockwise with time at any given height and also rotate clockwise with height at any given time. This is the sense of rotation corresponding to an upward propagating wave with $c > \bar{u}$ or a downward propagating wave with $c < \bar{u}$ in the Northern Hemisphere. Estimates of $\bar{u}$ by direct observation and $\bar{u} - c$ from equation 1 reveal that $c > \bar{u}$, implying upward energy propagation.

A quantitative picture of the wave came from least squares fitting of sine curves to the time series of radial velocities measured at each height in each beam is shown in Figure 2. These fits gave the amplitude and phase (or time of maximum) and the best fit period of the wave. The period was found to be 7 hrs. Combining the phase and amplitude parameters from the two orthogonal beams revealed the fact that the rotating wind vector traced out an ellipse with a maximum amplitude of 38 m/s horizontal with the major axis of the ellipse along a line from 50° to 230°. In principle, knowledge of the time of

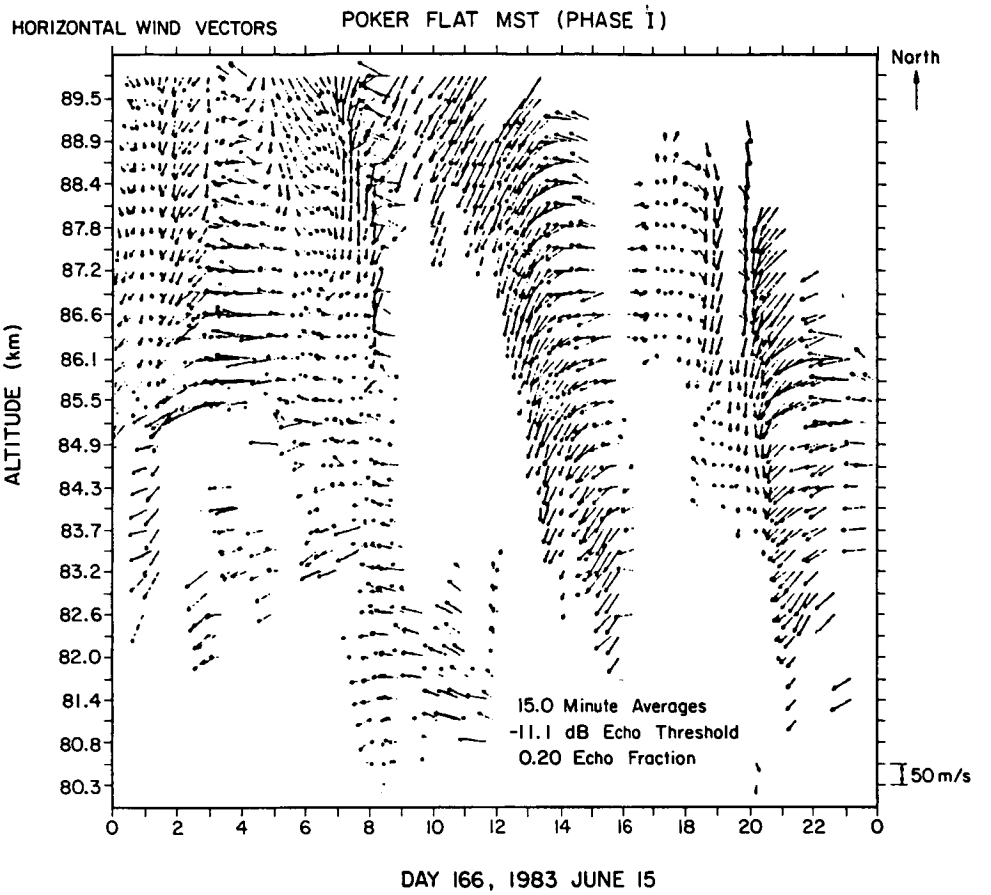

Figure 1. Time-height cross section of horizontal winds estimated from Poker Flat MST radar data. Blank spaces occur where the return signal was too weak to yield reliable wind estimates.

maximum vertical velocity would determine the direction of wave propagation but during the STATE campaign the Poker Flat MST radar's Doppler velocity resolution was insufficient to reliably measure the small vertical velocity component of this wave. The propagation direction was determined through use of the rocket data as will be mentioned below.

Measurement of the change of phase with height, apparent in Figure 2, led to an estimate of 19 km for the vertical wavelength of this wave. With our estimate for N of 0.03 rad/s from the rocket-measured temperature profile and the observed value for m, $\bar{u}$-c is found to be 90 m/s using the approximate dispersion relation. This implies that the wave amplitude is at about 40% of the saturation amplitude. Thus, it appears that this wave is not large enough, by itself, to produce the turbulent mixing of the electron-density gradient to which the MST radar is sensitive. However, the wave amplitude, shown in Figure 3, is not growing exponentially with height, implying that some of the wave energy is being dissipated in the 82-89 km region.

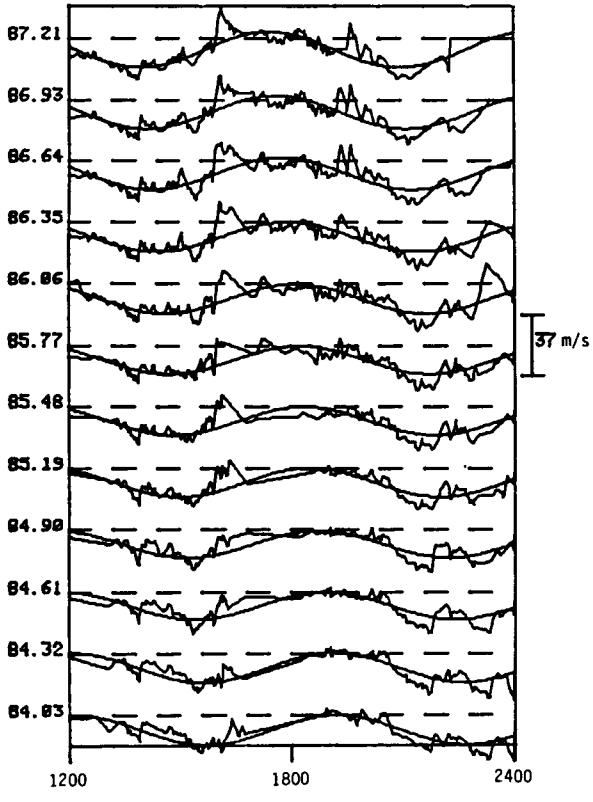

Figure 2. Time series of wind speeds measured along the east beam on June 15, 1983. Times are in Alaska Standard Time (local meridian time).

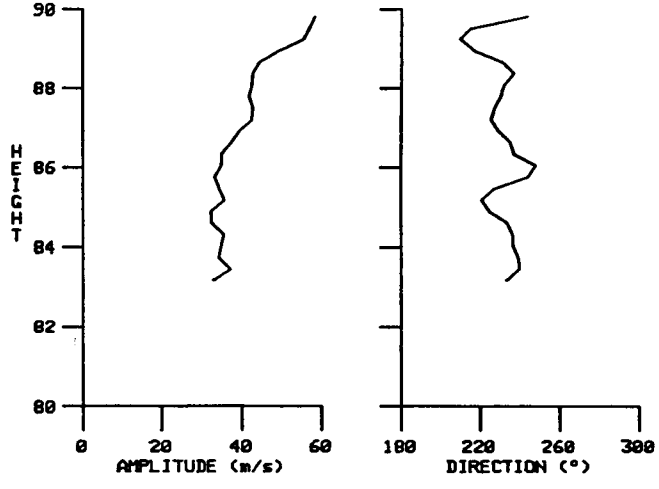

Figure 3. Estimated horizontal amplitude (u') and propagation direction profiles for the 7-hr wave.

NIKE-HYDAC ROCKET DATA

At 2051 AST on June 15, 1983, a Nike-Hydac rocket boosted an instrumented sphere to an altitude of about 75 km. The sphere continued in free flight to an altitude of 130 km. Data were obtained from both the upleg and downleg flights providing a continuous profile of winds and temperature from 75 to 130 km. The one instrument in the sphere relevant to this study was a 3-axis accelerometer used to measure accelerations due to density changes and changes in the winds. The temperature profile was obtained through integration of the measured density profile.

The resultant meosphere/lower thermosphere temperature profile is shown in Figure 4. There is a deep temperature minimum of 130°K at the summer mesopause near 86 km. The wind component profiles obtained from the accelerometers appear in Figure 5. Again, the presence of an inertio-gravity can be inferred from the wind data since the wind vector rotates clockwise with height above about 90 km.

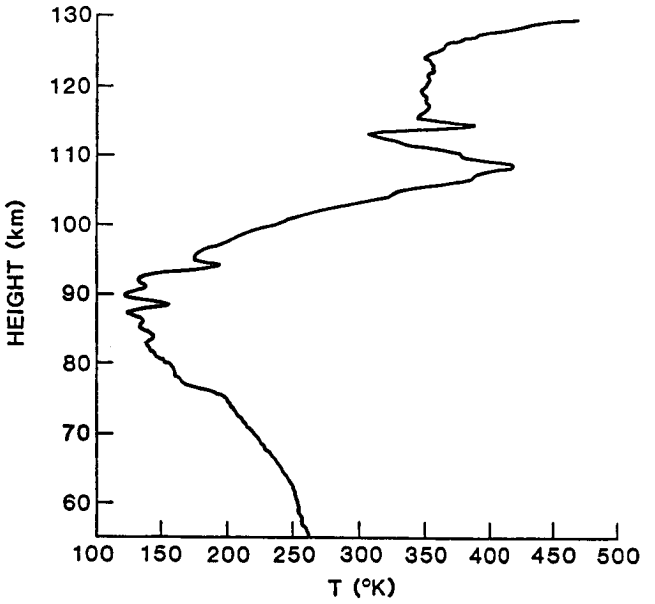

Figure 4. Temperature profile obtained by accelerometer sphere at 2055 AST, June 15, 1983. Note the cold summer mesopause with a temperature of 130°K near 86 km.

Before attempting to fit sine waves to the temperature and wind profiles, the data were differenced to remove linear trends such as the steady increase of temperature with height in the lower thermosphere. The differenced profiles appear in Figure 6. Fits were only made to the data above 85 km to avoid any influence the notch at the mesopause might have on wave amplitude or phase.

The best fit vertical wavelength was found to be 30 km. Combining the wave amplitudes and phases from the wind data led to the conclusion that a wave with an amplitude of 82 m/s was propagating towards 6° or 186°, with the maximum velocity occurring at 92 km. The propagation direction can be

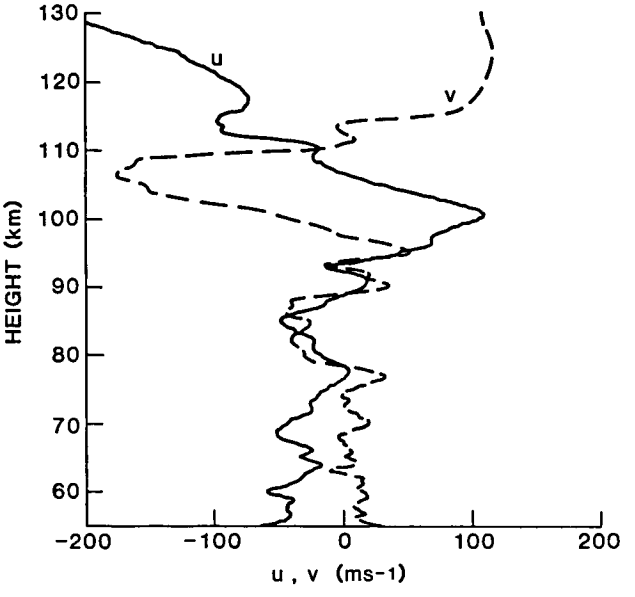

Figure 5. Wind profiles from the accelerometer sphere flight at 2055 AST, June 15, 1983. U is the zonal and V the meridional wind component.

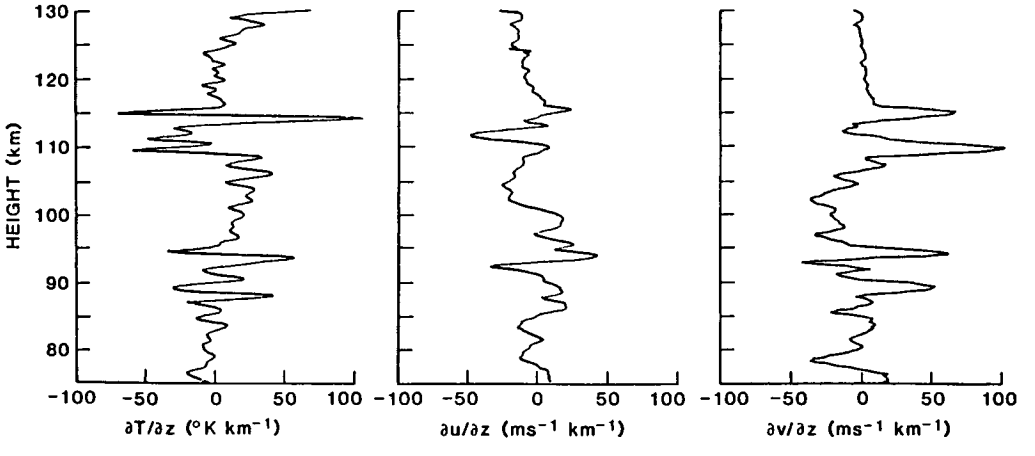

Figure 6. Differenced data from the profiles of Figures 4 and 5. Note the large variance in all three profiles at heights of 85 and 115 km.

determined through use of the temperature data and the fact that the most negative temperature gradient will occur at the height at which the perturbation velocity is in the direction of propagation. This occurred at 85 km where the wind vector is directed towards 295°. Thus, the two direction estimates from the rocket data bracket the direction inferred from the radar data. Uncertainties in the rocket data, principally the uncertainty introduced when removing the linear trend in the velocity profiles without actually knowing the mean wind profile, produce large uncertainties in the wave direction. However, the location of the most negative temperature gradient coincides with a wave velocity maximum in the radar data directed towards 230°. This fact and the nearly constant propagation direction profile in Figure 3 suggest that 230° is the most probable direction of wave propagation.

The wave amplitude and $\bar{u}$-c inferred from the vertical wavelength imply the wave is near 75% of saturation amplitude. The percentage of saturation amplitude from the velocity estimates agrees rather well with the degree of saturation from the temperature measurements. The ratio of the perturbation temperature lapse rate to that of the mean plus adiabatic lapse rate gives a figure of 73% of saturation amplitude. The analysis by FRITTS and RASTOGI (1985) yields a saturation amplitude of 0.82 ($\bar{u}$ - c) due to the transverse shear of the wave and the corresponding decrease in the local Richardson number. Thus, this wave was very near saturation at upper heights. This seems to contradict the radar data that suggested the wave was at only 40% of saturation amplitude. However, the radar data are centered near 85 km while the wave parameters from the rocket data were computed for the region from 85 to 130 km. The wave amplitude increase with height is consistent with the radar data in Figure 3.

Another discrepancy between the two data sets is the vertical wavelength of 19 km from the radar data and 30 km from the rocket data. This difference is to be expected since the steep temperature gradient above the mesopause and larger values of N act to suppress vertical motion and lead to a compression of vertical wavelenghts relative to the less steep gradients and smaller values of N in the thermosphere as can be seen from the approximate dispersion relation (equation 1).

The wave parameters are summarized in Table I along with 95% confidence limits from the least squares fitting of sine waves. The larger values of $\bar{u}$ - c, in Table I come from use of a more complete dispersion relation than equation 1, which has been used in the preceding paragraphs.

DISCUSSION

Analysis has shown that both the rocket payload and the radar were observing the same low-frequency (7 hr period), long-wavelength (19-30 km), large-amplitude (.4 - .8 of saturation amplitude) inertio-gravity wave. Both data sets also exhibit manifestations of wave saturation or breaking.

The variance of the difference profiles of Figure 6 is much greater at heights of 85 and 115 km than elsewhere and this is true for all three profiles. These heights are also the heights at which the wave-induced temperature perturbation lapse rate is most negative and the atmosphere is most nearly unstable. The increased variance appears to be due to the presence of smaller scale wave activity.

The radar data show that the regions of greatest S/N coincide with the locations of the most unstable lapse rate and of the maximum velocity perturbation in the direction of wave propagation as can be seen in Figure 7. The contours are of S/N averaged over both oblique beams. The solid lines mark

Table I

Large-scale wave characteristics on June 15, 1983

	Radar data	Rocket data
Data window	1200-2400 AST 82 - 89 km	2055 AST 85 - 130 km
Period	7 hr	
λ_z	19 km	30 km
u'	38 $\pm$ 5 m/s	82 $\pm$ 9 m/s
T'		59 $\pm$ 5°
T' (using u' and polarization relations)	20°	69°
propagation dir.	230 $\pm$ 10°	186 or 295 $\pm$ 55°
assumed N	0.03 rad/s	0.023 rad/s
$\bar{U} - c$	121 m/s	110 m/s
c	151 m/s	
$u' / \bar{U} - c$	0.26	0.75
$T_z' / (\bar{T}_z + g/c_p)$		0.73
u' / v'	1.48	1.98
intrinsic period using $\bar{U} - c$ using u'/v'	 8.74 hr 9 hr	 6.67 hr

the location of the most negative temperature gradient determined from the rocket temperature data (to be at 85.4 km at 2055 AST) and the vertical phase speed estimated from the radar data. Clearly, the largest radar signal strengths (and presumably the largest 3 m turbulence intensity) come from regions determined by the near saturation of the inertio-gravity wave. Recall that the single wave by itself was not large enough to saturate and produce turbulence, but FRITTS (1985) reported a numerical simulation demonstrating that a superposition of waves can lead to saturation, even though none of the waves possess saturation amplitude independently. Thus, gravity-wave saturation near the mesopause involves a broad spectrum of internal gravity waves.

This phenomenon of largest S/N appearing where the wave field is most nearly unstable and also where the perturbation velocity vector is in the direction of wave propagation allowed the determination of wave parameters for a 3-hr period wave on June 17, for which temperature measurements were not available.

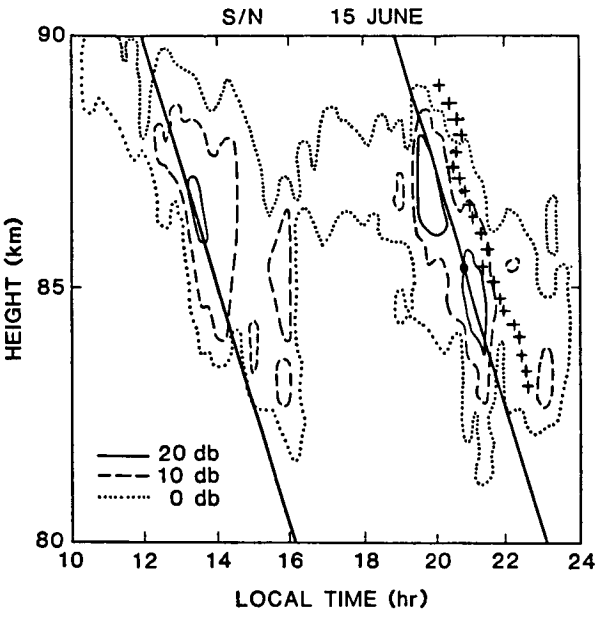

Figure 7. Contours of S/N averaged over both oblique radar beams. Crosses are locations of the maximum amplitude of the 7-hr inertio-gravity wave. Dot at 85 km is location of most unstable lapse rate from rocket data and solid line indicates motion of that lapse rate with the phase speed of the 7-hr wave.

Both of these cases imply that the regions of intense mixing of the electron-density gradient are closely coupled to the saturation of large-scale inertio-gravity waves. The scenario developed by BALSLEY et al. (1983) of gravity waves being vertically compressed as they approach the summer mesopause and thus approaching instability thresholds, holds for the inertio-gravity waves observed during STATE.

This study has benefited tremendously from the combined data sets obtained by rocket and MST radar. Future analysis of mesospheric dynamics and chemistry should involve different, yet complimentary data-acquisition methods, i.e., the radar provides a time history of winds while rockets provide a more extensive height profile of winds and temperature. Substituting a lidar for the rocket measurements would permit acquisition of a very complete picture of gravity-wave dynamics.

ACKNOWLEDGEMENTS

This work was supported by Air Force Office of Scientific Research (AFSC) under Grant AFOSR-82-0125. The preparation of this manuscript was expeditiously completed by the staff at CIRES.

REFERENCES

Balsley, B. B., W. L. Ecklund, and D. C. Fritts (1983), VHF echoes from the high-latitude mesosphere and lower thermosphere: Observations and interpretations, J. Atmo. Sci., 40, 2452-2466.

Fritts, D. C. (1984), Gravity wave saturation in the middle atmosphere: A review of theory and observations, Rev. Geophys. Space Phys., 22, 275-308.

Fritts, D. C. (1985), A numerical study of gravity wave saturation: Nonlinear and multiple-wave effects, J. Atmo. Sci., in press.

Fritts, D. C., and P. K. Rastogi (1985), Convective and dynamical instabilities due to gravity wave motions in the lower and middle atmosphere: Theory and observations, Radio Sci., 20, 1247-1278.

Hodges, R. R., Jr. (1967), Generation of turbulence in the upper atmosphere by internal gravity waves, J. Geophys. Res., 72, 3455-3458.

Philbrick, C. R., D. P. Sipler, B. B. Balsley, and J. C. Ulwick (1984), The STATE experiment - Mesospheric dynamics, in Adv. in Space Research, 4, 6, 129-132.